XI International Conference on Computational Plasticity. Fundamentals and Applications
COMPLAS XI
E. Oñate, D.R.J. Owen, D. Peric and B. Suárez (Eds)

THE INFLUENCE OF LOAD MISALIGNMENT ON FRP-CONCRETE BOND BEHAVIOUR, A NUMERICAL STUDY

P. NETO[*] AND J. ALFAIATE [†]

[*] Escola Superior de Tecnologia do Barreiro
Setubal Polytechnic Institute
Rua Stinville, nº 14, 2830-144 Barreiro, Portugal
e-mail: pedro.neto@estbarreiro.ips.pt, web page: http://www.estbarreiro.ips.pt

[†] ICIST, Department of Civil Engineering and Architecture
Instituto Superior Técnico, Technical University of Lisbon
Av. Rovisco Pais 1, 1049-001 Lisboa, Portugal
Email: alfaiate@civil.ist.utl.pt

Key words: Bond Behaviour, Fibre Reinforced Polymers (FRP), Concrete, Fracture Energy in Modes I and II.

Abstract. Various authors have used pure shear test models in order to describe the bond between FRP and concrete. However, considerable dispersion of the parameters which characterize the bond behaviour has been found. In pure shear models it is assumed that the load applied to the FRP is parallel to the axis of the concrete specimen and acts on the plane of symmetry. In this work, a numerical model is presented to analyse the influence of load misalignment on FRP-concrete bond behaviour.

1 INTRODUCTION

The use of fibre reinforced polymers (FRP) applied to the external strengthening of concrete structures, in particularly the use of laminates and sheets, has become an increasingly common practice. This is due, namely, to the mechanical properties of these composite materials, such as the ease of application and high strength-to-weight ratio. The major problems found with this reinforcement technique are the local failure modes. In the last few years, several experimental and analytical studies have been carried out, which contributed to the understanding and quantification of the phenomenon related to the bond behaviour between concrete and FRP. However, several issues still need to be clarified.

Various authors [1, 2, 3, 4, 5, 6] used pure shear test models in order to describe the bond behaviour, which contributed to the definition of constitutive relationships for the interface concrete-FRP. A considerable dispersion of the parameters adopted to characterize the bond behaviour has been found [7].

In pure shear models it is assumed that: i) the load applied to the FRP is aligned with the axis of the concrete specimen and ii) the load is applied at the symmetry axis of the strengthened material. In this work, the influence of a deviation angle of the load with respect to the element axis is analysed. A numerical model is presented, based on previous studies [7, 8, 9], in which the stress distribution long the interface concrete-FRP is evaluated. These

stresses can be both tangential and normal to the interface. In this study, unidirectional carbon fibres sheets are considered.

The bond between the FRP and the concrete is modelled using a discrete crack approach, based on Non-Linear Fracture Mechanics [10]. Interface elements with zero initial thickness are adopted. The shear and peeling stresses developed at these elements are dependent on the relative displacements measured between the strengthening material and the concrete surface, according to a local constitutive relationship under softening. The material properties that characterize the interface, namely the shear and peeling stiffness, the cohesion, the tensile strength and the fracture energy in modes I and II, are obtained from previous works [7, 8, 9]. From the analysis of the results numerically obtained, it is possible to draw conclusions concerning the relative importance of each parameters and the influence of the load slope on the obtained results. It is expected that this work may contribute to identify some aspects which should be considered in a setup of experimental tests and to clarify the interpretation of the results obtained from those tests.

2 PURE SHEAR MODEL

The pure shear model considered in this work consisted of concrete specimens in which unidirectional carbon fibres were glued, by means of resin epoxy. The specimen was subjected to a tensile load along the direction of the fibres, as shown in Figure 1. This model was used in previous studies [11]. The concrete specimens tested were 400mm long and had a rectangular cross-section of 200mm by 200mm. The strengthening material had a width of 80mm and was applied on the larger face of the specimen. The nominal values for Young's modulus and for the ultimate tensile strain of the CFRP were 240GPa and 1.55%, respectively. Mean values of 36.4MPa, 2.8MPa and 31.6GPa, for the compressive strength, tensile strength and Young's modulus of concrete, respectively, were considered.

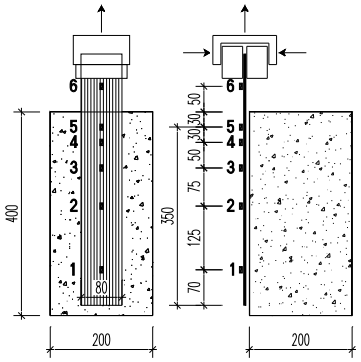

Figure 1: Shear model on concrete joint strengthened externally by CFRP [11]

3 MATERIAL MODEL

The concrete is assumed a continuum exhibiting an isotropic linear elastic behaviour. The FRP behaviour is assumed linear elastic until failure. The bond between concrete, resin and CFRP is modelled using interface elements of zero initial thickness and a discrete crack approach.

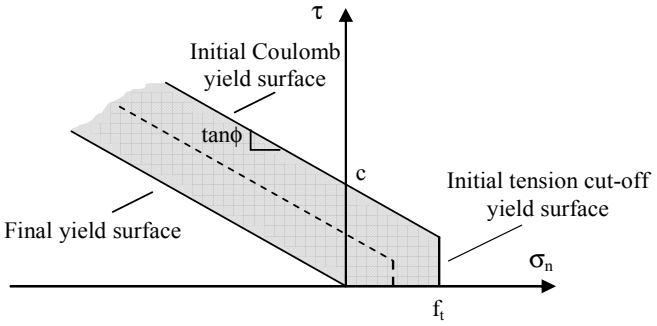

Figure 2: Yield surfaces adopted for the interface

A multi-surface plasticity model is adopted [12, 13]; two limit surfaces are considered: a tension cut-off for mode-I fracture and a Coulomb friction envelope for mode-II failure and mixed mode, as shown in Figure 2. In this figure, the horizontal axis represents the normal stress vector component and the vertical axis represents the tangential stress vector component measured at the interface. The cut-off mode-I is defined by the tensile strength of the concrete. The Coulomb friction envelope is initially characterized by the cohesion coefficient and by the internal friction angle ϕ. Both yield functions follow exponential softening flow rules (Figure 3).

The yield function associated with the normal stress is given by:

$$f_n = \sigma_n - f_t \exp\left(-\frac{f_t}{G_F^I} w\right) \tag{1}$$

where σ_n is the stress vector component measured at the interface. An associated flow rule is considered. The shear yield function reads:

$$f_s = |\tau| + \sigma_s \tan\phi - c \cdot \exp\left(-\frac{c}{G_F^{II}} s\right) \tag{2}$$

where τ is the tangential stress vector component measured at the interface. A non-associated flow rule is adopted with a plastic potential g_s given by:

$$g_s = |\tau| + \sigma_n \tan\psi - c \tag{3}$$

where ψ is the dilatancy angle. An isotropic softening criterion is adopted, meaning that both yield surfaces shrink the same relative amount in the stress space, and both keep the origin (Figure 2).

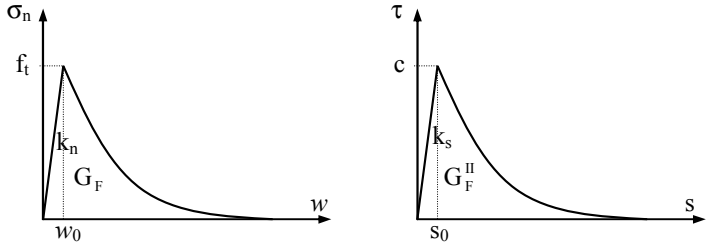

Figure 3: Normal and tangential constitutive relationships adopted for the interface

The material parameters characterizing the interface behaviour are: the elastic shear and peeling stiffness, k_s and k_n, respectively, the cohesion c, the tensile strength f_t, and the fracture energies in modes I and II, G_F and G_F^{II}, respectively (area under the curves σ_n-w and σ_s-s adopted as shown in Figure 3).

4 NUMERICAL ANALYSIS

The numerical analysis is performed using the finite element method [7]. Considering the very high stiffness of the concrete when compared to the epoxy and the FRP, this material is modelled by rigid supports. For the strengthening material, except in the reference models, 4 node isoparametric elements are adopted. These elements allow the bending stiffness of the composite to be considered. For the FRP, in the reference models, linear 2-node elements are considered [7]. The bond behaviour is modelled by linear interface elements with initial zero thickness.

The specimen response is determined under displacement control, using an incremental, iterative procedure.

As mentioned above, the constitutive relationship of the interface concrete-CFRP is defined by six parameters: the shear and peeling stiffness, the cohesion, the tensile strength and the fracture energy in modes I and II.

According with previous studies [7, 9] the following values are adopted: k_s=1500MPa/mm and k_n=4000MPa/mm, for the shear and peeling stiffness, respectively, c=5MPa for the cohesion and G_F^{II}=1.5N/mm for the fracture energy in mode II. In the case of fracture energy in mode-I there is a large variation on the values proposed in the bibliography [4, 14, 15, 16, 17], namely in the relationship between G_F^{II} and G_F. A value of G_F=0.1N/mm is considered assuming a relation G_F^{II} /G_F between 10 and 25 [4, 14, 15].

The angle α is defined between the direction of the applied force and the y axes of the model (corresponding to the fibre orientation), in order to define the load slope: α=0º, as well as values of α>0º and α<0º are adopted, meaning a counter clockwise and clockwise rotation, respectively, with respect to the fibre axis. In this study the following values are used: α=±1.0º and α=±0.5º. The load deviation with respect to the fibre orientation is implemented by means of the corresponding components: one along the direction of the fibres and the other perpendicular to the strengthening material. As a consequence, in addition to the stresses tangential to the interface, normal stresses are expected to develop.

Next, the numerical study is presented. In the analysis, the adopted thicknesses of the CFRP are: t_f=0.5mm and t_f=0.1mm. These values are typical of CFRP sheets.

4.1. CFRP thickness equal to 0.5mm

For a composite thickness of 0.5mm and α=+1.0º the interfacial stress distribution along the bond length is obtained. In Figures 4 and 5, the interfacial stresses along the bond length for several load levels are presented, for applied loads close to 20% and 90% of the maximum load registered in that model, which is circa 48kN.

For lower load levels, some values of the shear stresses are higher than the cohesion defined due to the presence of normal compressive stresses, which is in according with the yield surface adopted as shown in Figure 2. These stresses only occur along a small length, near the location where the load is applied. Apart from the region where normal stresses co-

exist, the shear stress distribution becomes similar to the one obtained in a pure shear model [7].

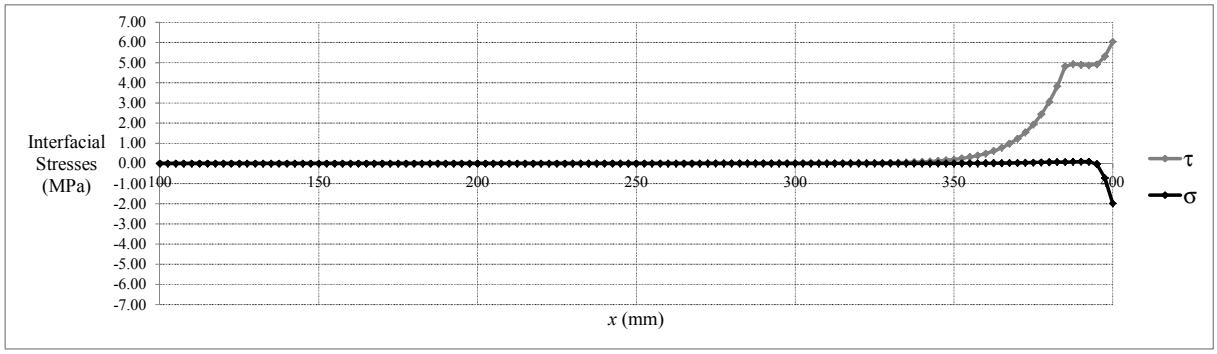

Figure 4: Interfacial stresses with t_f=0.5mm, F=10kN and α=+1.0º

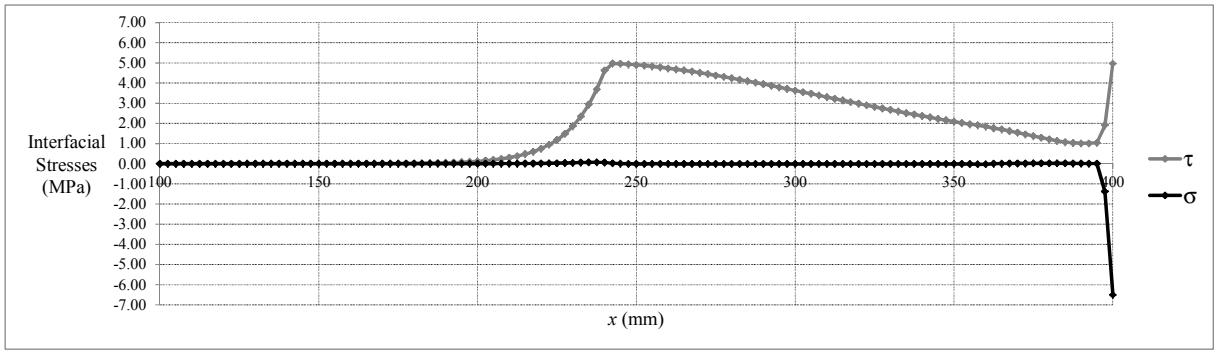

Figure 5: Interfacial stresses with t_f=0.5mm, F=43kN and α=+1.0º

In Figures 6 and 7, the interfacial stresses along the bond length for several load levels are presented, for applied loads close to 20% and 90% of the maximum load registered in that model when α=−1.0º, which was circa 25kN. Except in the region where normal stresses co-exist, the shear stress distribution becomes once more similar to the one obtained in a pure shear model [7]. Also in this case it is possible to observe normal stresses to the interface in addition to the tangential stresses. These stresses are mainly peeling stresses and also occur along a small length near the location where the load is applied. Thus, conversely to the previous case, shear stresses above the cohesion are not found.

With α=−1.0º, the maximum load is circa 52% of the maximum load obtained in the case with α=+1.0º. Theoretically, this relationship should be close to 100%. Since the evaluation of the mode-II fracture energy based on experimental tests is much dependent from the ultimate load, it is important to mention that unreliable values of this parameter will be obtained if α in the experimental setup is less than zero. This issue will be further discussed below.

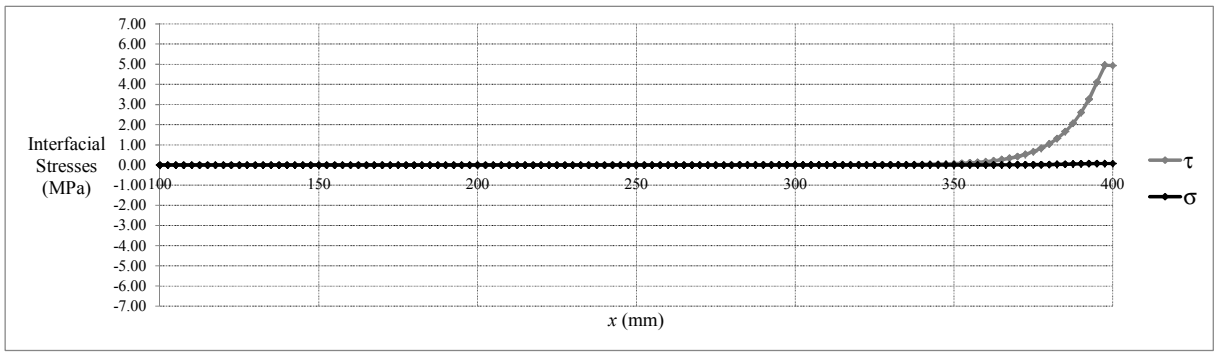

Figure 6: Interfacial stresses with t_f=0.5mm, F=5kN and α=−1.0º

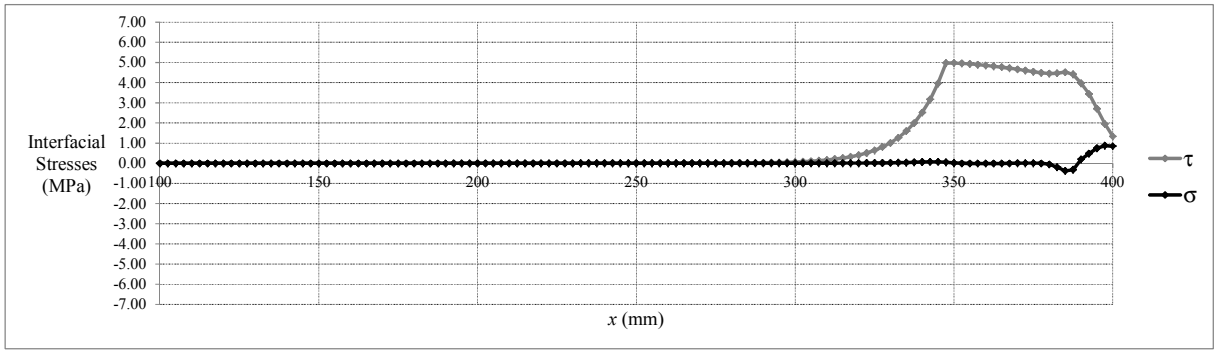

Figure 7: Interfacial stresses with t_f=0.5mm, F=22.5kN and α=−1.0º

The results obtained with α≠0º and with α=0º for a load level of 65% of the maximum load obtained with α=+1.0º and α=−1.0º, 31kN and 16kN, respectively, are compared and presented in Figures 8 and 9.

From the analysis of the results obtained from the two models, with α=+1.0º and α=0º, it is found that the corresponding maximum load and the shear stress distribution are similar, as shown in Figure 8, except along a small length near the location where the load is applied. The experimental results obtained with α=+1.0º allow for the satisfactory quantification of the material parameters that define the constitutive law of the bond behaviour between concrete and CFRP, namely: k_s, c and G_F^{II}.

The shear stress distributions obtained with both α=−1.0º and α=0º are similar, for a load of 16kN, as can be observed in Figure 9. However there are some differences which should be noticed. The relation between the maximum loads with α=−1.0º and with α=0º is about 52%. This is a very important aspect because it has direct implications on the value which could be adopted, by mistake, for G_F^{II}. The maximum load in the model with α=−1.0º is 25kN. From this result, the fracture energy in mode II was estimated according to Equation (4) [7, 18, 19]. The obtained value was 0.41N/mm, which is about 27% of the reference value, considering a pure shear model.

A new pure shear model was defined considering the above obtained value for the fracture energy in mode-II: G_F^{II}=0.41N/mm. Values of c=5.0MPa and k_s=1500MPa/mm were adopted for a complete definition of the interface behaviour. The results from this model, called α1=0, are shown in Figure 9. As expected, from this figure it is possible to observe a very good

agreement between the stress distribution and the maximum load obtained from both models: with α=−1.0º and α1=0º. However, these "corrected" values of fracture energy, obtained with α=−1.0º, are not the right ones.

$$N_u = b_f \times \sqrt{2E_f \times t_f \times G_F^{II}} \tag{4}$$

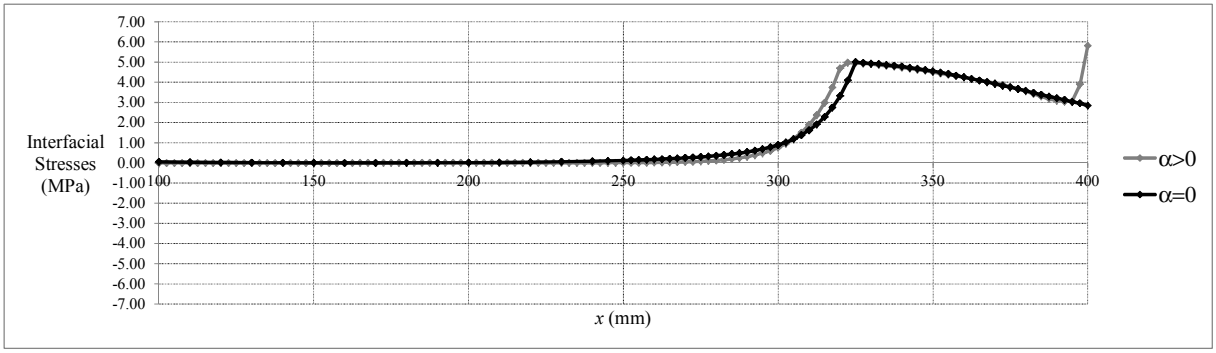

Figure 8: Shear stresses with t_f=0.5mm and F=31kN

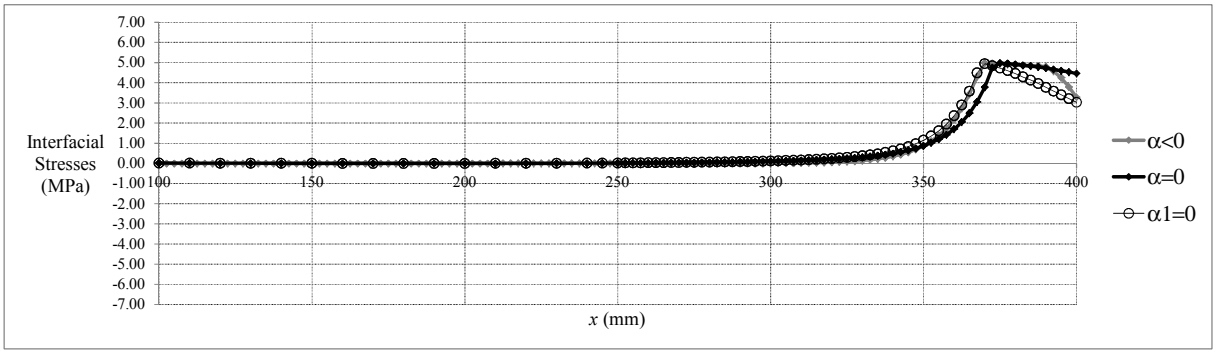

Figure 9: Shear stresses with t_f=0.5mm and F=16kN

Considering now a value of α equal to half of the previous, it is possible to note similar shear stress distribution as shown in Figure 10. However, the maximum load obtained from the model with α=−0.5º was 35kN, higher than 25kN which was obtained with α=−1.0º.

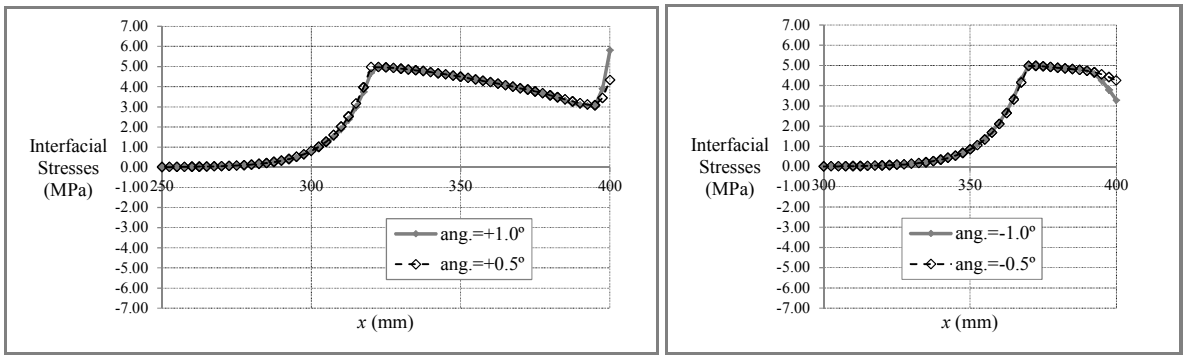

Figure 10: Shear stresses with t_f=0.5mm: F=31kN (ang.>0) and F=16kN (ang.<0)

4.2 CFRP thickness equal to 0.1mm

For a composite thickness of 0.1mm and α=+1.0º the interfacial stresses distribution along the bond length was obtained. In Figures 11 and 12, the interfacial stresses concrete-CFRP along the bond length are presented for several load levels, namely about 20% and 90% of the maximum load registered in that model, which was circa 22.5kN. From these figures it is possible to notice, as observed in the previous case with t_f=0.5mm, non-zero normal stresses. The normal stresses are compressive and occur along a smaller length than the one observed with t_f=0.5mm, next to the location where the load is applied. Except in the region where normal stresses co-exist, the shear stress distribution becomes similar to the one obtained in a pure shear model [7].

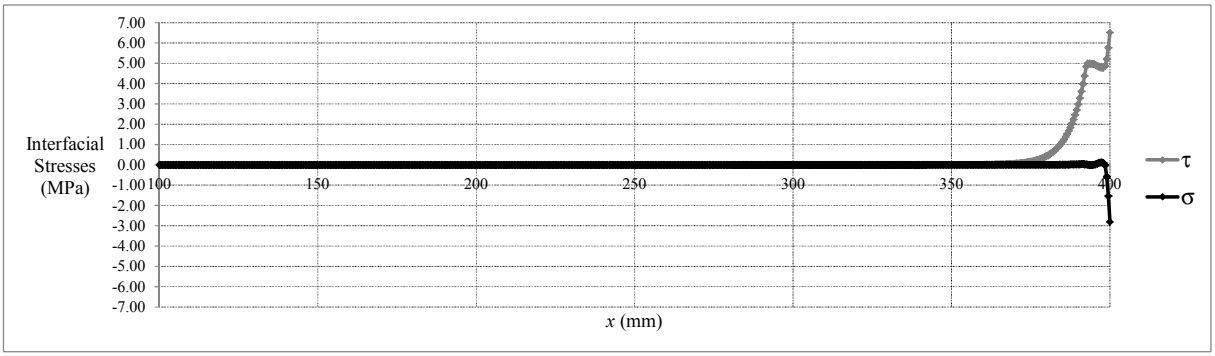

Figure 11: Interfacial stresses with t_f=0.1mm, F=5kN and α=+1.0º

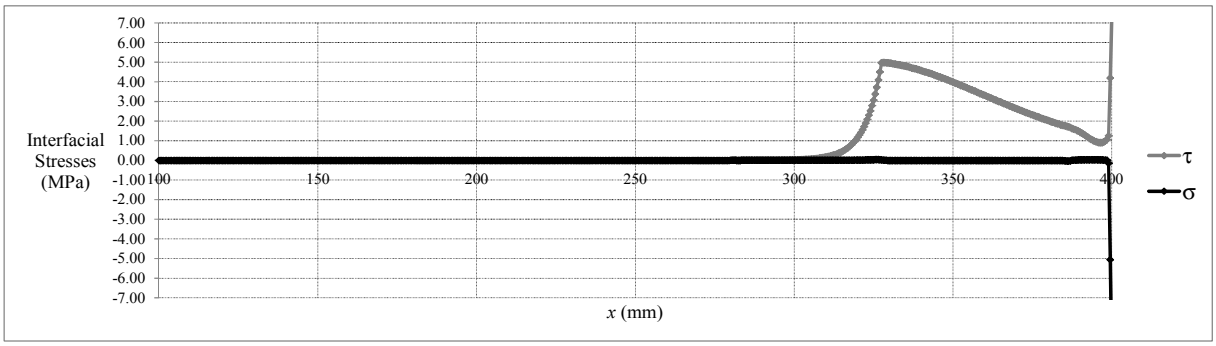

Figure 12: Interfacial stresses with t_f=0.1mm, F=20kN and α=+1.0º

In Figures 13 and 14, for α=−1.0º, the interfacial stresses along the bond length are presented for several load levels similar to the values previous adopted, namely about 20% and 90% of the maximum load registered in that model, which was circa 9.5kN. For t_f=0.1mm the relationship between the maximum load with α=−1.0º and α=0º is circa 42% and for t_f=0.5mm the corresponding ratio is 52%. Thus, compared to the case α=0º, the decrease of the maximum load under α<0º seems to become more significant when the external reinforcement thickness decreases. Similar to the case with t_f=0.5mm, the value of the fracture energy in mode-II obtained from an experimental test in these conditions will hardly match the theoretically correct one.

Except in the region where normal stresses co-exist, the shear stress distribution becomes similar to the one obtained in a pure shear model. Also in this case it is possible to observe

normal stresses to the interface in addition to the tangential stresses. The normal stresses, mainly peeling stresses, only occur along a small length, next to the location where the load is applied.

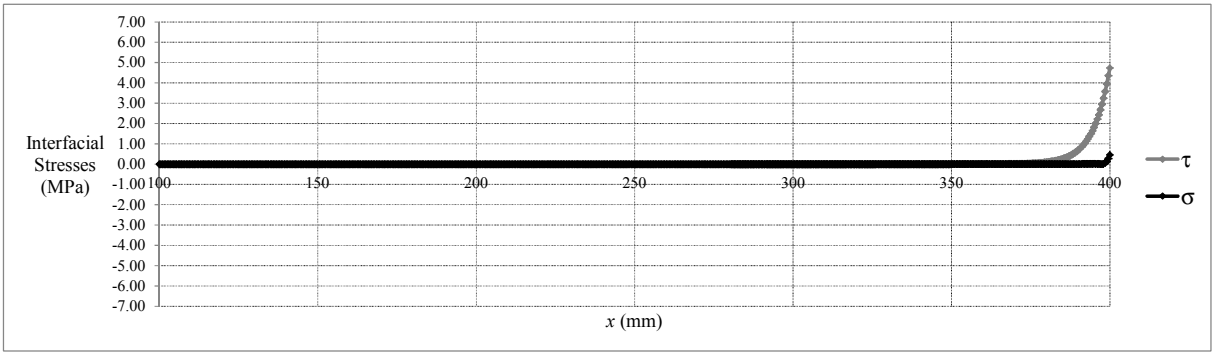

Figure 13: Interfacial stresses with t_f=0.1mm, F=2kN and α=−1.0º

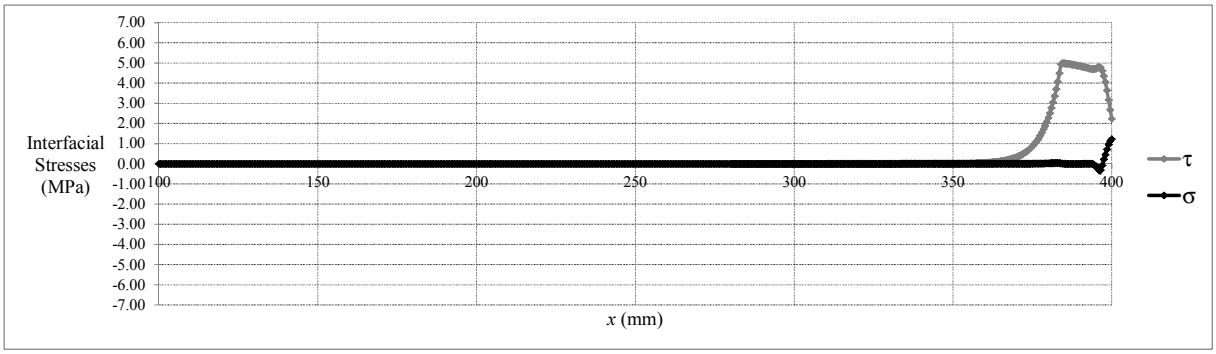

Figure 14: Interfacial stresses with t_f=0.1mm, F=8kN and α=−1.0º

An analysis similar to the previous one adopting t_f=0.5mm was performed. The results obtained with α≠0º and α=0º for a load level of 65% of the maximum load obtained with α=+1.0º and α=−1.0º, 15kN and 6kN, respectively, are presented in Figures 15 and 16.

From the analysis of the results obtained from the two models, with α=+1.0º and α=0º, it is found that the corresponding maximum load and the shear stresses distribution are almost coincident, as shown in Figure 15. Thus, in this case, the experimental results with α=+1.0º allow for a good quantification of the material parameters that define the constitutive law of the bond behaviour between concrete and CFRP, namely: k_s, c and G_F^{II}.

The shear stress distributions obtained with α=−1.0º and α=0º are similar, for a load of 6kN, as can be observed in Figure 16. However there are some differences that should be noticed. The relationship between the maximum loads with α=−1.0º and with α=0º is about 42%. As mentioned above, this is a very important aspect because it has direct implications on the value to be considered for G_F^{II}. The maximum load in the model with α=−1.0º is 9.5kN. From this result, the fracture energy in mode II was estimated according to Equation (4). The obtained value was 0.26N/mm, which is about 17% of the reference value, considering a pure shear model. In this case, the obtained G_F^{II} value would be even farther from the reference value than the value obtained considering t_f=0.5mm. A new pure shear

model was defined adopting G_F^{II}=0.26N/mm and the reference values: c=5.0MPa and k_s=1500MPa/mm. The results from this model, called by α1=0, are shown in Figure 16. As expected, from this figure it is possible to observe a good agreement between the stress distribution and the maximum loads obtained from both models: with α=−1.0º and α1=0º. Nevertheless, this "corrected" value of the fracture energy, obtained with α=−1.0º, is definitely not the right one.

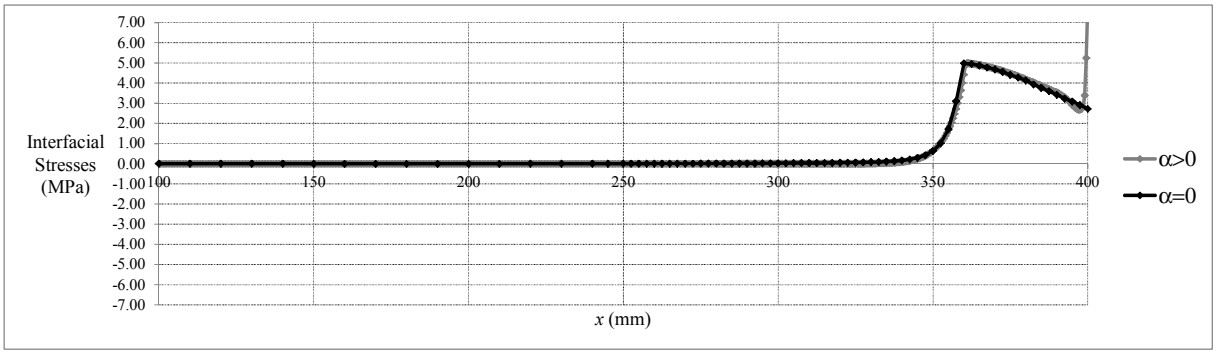

Figure 15: Shear stresses with t_i=0.1mm and F=15kN

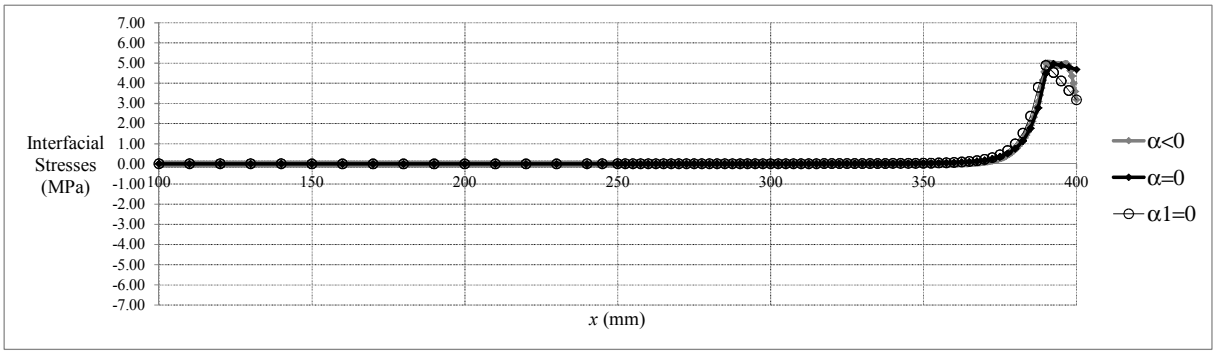

Figure 16: Shear stresses with t_i=0.1mm and F=6kN

5 CONCLUSIONS

In shear tests, adopting a deviation of the load orientation with respect to the FRP fibre orientation (α≠0º), normal stresses are obtained in addition to the stresses tangential to the interface, whereas no normal stresses occur in a pure shear model.

Considering α>0 and especially for higher thickness values, the maximum tangential stress tends to be higher than the cohesion along a small bond length, due to the existence of normal compressive stresses in the interface, in particularly for lower load levels. This small length, near to the beginning of the glued joint where the load is applied, tends to decrease with the thickness adopted.

Except in the region where normal stresses co-exist, the shear stress distribution becomes similar to the one obtained in a pure shear model.

Considering the maximum load, if α>0, its value is close to the value obtained from a pure shear test. However, if α<0, due to the existence of normal stresses at the interface, a significant reduction of the bond strength is observed, which seems to be more pronounced

using smaller FRP thickness. In this case, the measured fracture energy in mode-II is significantly different from the theoretically correct value.

The normal stresses under $\alpha<0$ are mainly peeling stresses, which occur along a small length.

With regard to the quantification of the material parameters, which define the behaviour of the bond between concrete-FRP, it is possible that these load misalignments, in an experimental shear test setup, may be responsible for the large dispersion observed in several works [7], namely:

i) the evaluation of fracture energy in mode-II based on these tests is very sensitive to the load misalignment, mainly if $\alpha<0$;
ii) the cohesion quantification from experimental tests could be accurately achieved. However, some attention should be paid to the possibility of obtaining shear stresses higher than the cohesion, along a small length, due to load misalignment;
iii) the shear stiffness appears as the parameter with the largest range of values when compared to the cohesion and the fracture energy in mode-II. However, this parameter essentially depends on the adhesive [7] and for larger values its influence, in the maximum load and in the tangential stresses, could be neglected.

It is important to stress that, if the imperfection related to the experimental test corresponds to $\alpha<0$, the obtained maximum load value can be less than half the value obtained from a test with $\alpha=0$ or $\alpha>0$.

As shown, the results obtained with $\alpha>0$ are considerably closer to the ones resulting from a pure shear test than the values obtained with $\alpha<0$.

When comparing the cases where $\alpha=+1.0^{\circ}$ and $\alpha=+0.5^{\circ}$ no significant differences are registered. However, with a negative angle, a significant difference is found, since the maximum load varies from 35kN to 25kN when the angle varies from 0.5° to 1.0°.

As a final remark, the material thicknesses considered in this study are typical from fibre carbon sheets. Thus, it is possible that the use of laminates proves to be less sensitive to the variation of the load direction.

ACKNOWLEDGEMENT

Financial support has been provided by the Portuguese Fundação para a Ciência e a Tecnologia (FCT) of the Portuguese Ministry of Science and Technology and Higher Education (PROTEC 2009).

REFERENCES

[1] Xue, W., Zenga, L. and Tana, Y. Experimental studies on bond behaviour of high strength CFRP plates, *Composites Part B: Engineering* (2008) 39(4), 592-603.
[2] Mazzotti, C., Savoiaa, M. and Ferracutia, B. An experimental study on delamination of FRP plates bonded to concrete, *Construction and Building Materials* (2008) 22(7), 1409-1421.
[3] Malek, A.M., Saadatmanesh, H. and Mohammad, R.E. Prediction of failure load of RC beams strengthened with FRP plate due to stress concentration at the plate end, *Structural Journal, ACI* (1998) 95(2), 142-152.

[4] Täljsten, B. *Plate bonding – strengthening of existing concrete structures with epoxy bonded plates of steel or fibre reinforced plastics*, Doctoral Thesis, Division of Structural Engineering, Lulea University of Technology, (1994).
[5] Chajes, M.J. and Finch jr., W.W., Januszka, T.F. and Thomson jr., T.A. Bond and force transfer of composite material plates bonded to concrete, *Structural Journal, ACI*, (1996) 93(2), 208-217.
[6] Bizindavyi, L. and Neale, K.W. Transfer lengths and bond strengths for composites bonded to concrete, *Journal of Composites for Construction, ASCE*, (1999) 3(4), 153-160.
[7] Neto, P. *Estudo numérico da ligação betão-CFRP*, Tese de Mestrado, Instituto Superior Técnico, Universidade Técnica de Lisboa, (2006).
[8] Neto, P., Alfaiate, J., Almeida, J.R. and Pires, E.B. The influence of mode-II fracture on concrete strengthened with CFRP, *Computers & Structures* (2004) 82(17-19), 1495-1502.
[9] Neto, P., Alfaiate, J. and Vinagre, J. Modelling the behaviour of reinforced concrete beams strengthened with FRP, *Proceedings of III European Conference on Computational Mechanics. Solids, Structures and Coupled Problems in Engineering, ECCM2006*, Laboratório Nacional de Engenharia Civil, Lisboa, Portugal, (2006).
[10] Hillerborg, A., Modeer, M. and Petersson, P.E. Analysis of crack formation and crack growth in concrete by means of fracture mechanics and finite elements, *Cement and Concrete Research* (1976) 6, 773-782.
[11] Travassos, N.C. *Caracterização do comportamento da Ligação CFRP-betão*, Tese de Mestrado, Documento provisório, Instituto Superior Técnico, Lisboa, Universidade Técnica de Lisboa, (2001).
[12] Lourenço, P.B. and Rots, J.G. A multi-surface interface model for the analysis of masonry structures, *Journal of Engineering Mechanics, ASCE* (1997) 123(7), 660-668.
[13] Alfaiate, J. and Almeida, J.R., Crack Evolution in Confined Masonry Walls, Idelshon, S.R., Oñate, E. and Dvorkin, E. eds. *Computational Mechanics: New Trends and Applications, CIMNE*, Barcelona, Spain, (1998).
[14] Bazant, Z.P. and Pfeiffer, P.A. Shear fracture tests of concrete, *Materials and Structures* (1986) 19, 111-121.
[15] Ozbolt, J., Reinhardt, H.W. and Xu, S. Numerical studies of the double-edge notched mode-II geometry, Mihashi, H. and Rokugo, K. eds. *FRAMCOS-3*, Japan, (1998) 2, 773-782.
[16] Alfaiate, J. and Pires, E.B. Mode-I and mixed-mode non-prescribed discrete crack propagation in concrete, Mihashi, H. and Rokugo, K. eds. *FRAMCOS-3,* Japan, (1998) 2, 739-748.
[17] Gálvez, J.C., Cendón, D.A., Planas, J., Guinea, G.V. and Elices, M. Fracture of concrete under mixed loading - experimental results and numerical prediction, Mihashi, H. and Rokugo, K. eds. *FRAMCOS-3,* Japan, (1998) 2, 729-738.
[18] Yuan, H., Wu, Z.S. and Yoshizawa, H. Theoretical solutions on interfacial stress transfer of externally bonded steel/composite laminates, *Journal of Structural Mechanics and Earthquake Engineering*, *JSCE* (2001) 675/I-55, 27-39.
[19] Wu, Z.S. and Niu, H.D Shear transfer along FRP-concrete interface in flexural members, *Journal of Material, Concrete Structures and Pavements*, *JSCE* (2000) 49(662), 231-245, 2000.